In Vivo Imaging

Enzymatically Shifting Nitroxides for EPR spectroscopy and Overhauser-Enhanced Magnetic Resonance Imaging

Gérard Audran,* Lionel Bosco, Paul Brémond,* Jean-Michel Franconi, Neha Koonjoo, Sylvain R. A. Marque,* Philippe Massot, Philippe Mellet,* Elodie Parzy, and Eric Thiaudière*

In memory of J.-P. Finet

Abstract: *In vivo investigations of enzymatic processes using non-invasive approaches are a long-lasting challenge. Recently, we showed that Overhauser-enhanced MRI is suitable to such a purpose. A β-phosphorylated nitroxide substrate prototype exhibiting keto–enol equilibrium upon enzymatic activity has been prepared. Upon enzymatic hydrolysis, a large variation of the phosphorus hyperfine coupling constant ($\Delta a_P = 4\ G$) was observed. The enzymatic activities of several enzymes were conveniently monitored by electronic paramagnetic resonance (EPR). Using a 0.2 T MRI machine, in vitro and in vivo OMRI experiments were successfully performed, affording a 1200 % enhanced MRI signal in vitro, and a 600 % enhanced signal in vivo. These results highlight the enhanced imaging potential of these nitroxides upon specific enzymatic substrate-to-product conversion.*

In recent years, dynamic nuclear polarization (DNP) has experienced a revival owing to bisnitroxide molecules as they can afford a dramatic NMR signal enhancement.[1] However, its application in vivo is still severely limited owing to its lack of selectivity toward biological processes. Furthermore, because the resonance frequency of the free electron is 660 times higher than that of the proton, free electrons require irradiation with high frequencies. Those are hardly compatible with imaging in living animals because the energy deposition is too high and wave penetration too shallow. In parallel, in the field of molecular imaging, anatomical magnetic resonance imaging (MRI) is growing into one of the most powerful non-invasive techniques for its high contrast in deeply-seated soft tissues, good spatial and temporal resolution, and its ability to diagnose pathological conditions. Nevertheless, the lack of sensitivity and non-selective contrasting agents hampers the use of MRI, particularly in the study of enzymatic processes occurring in vivo.

Proteases are a family of enzymes with a large variety of potential for diagnosis. Proteolytic activity is tightly regulated in space and time in normal tissues and thus is kept at low level and for short periods of time. However, they exhibit a persistent and specific activity in a number of diseases, such as solid tumors, pancreatitis, chronic obstructive pulmonary disease, cystic fibrosis, rheumatoid arthritis, and many inflammatory situations. Imaging these activities would offer an opportunity for early diagnosis independent of the anatomical alterations, which often appear later.[2–5] Recently, our groups highlighted the potential of the OMRI technique[6,7] at 0.2 T to detect and visualize a naturally occurring proteolytic activity in the digestive tract of living mice.[8–10] Herein, our new approach requires a nitroxide probe exhibiting changes in the hyperfine coupling constant larger than one Gauss upon enzymatic hydrolysis. To our knowledge, no nitroxides exhibit such a large frequency shift upon chemical or biological changes at physiological pH and temperature.[11–16] Previous reports of the use of nitroxides as probes relied on the changes in the nitrogen hyperfine coupling constant a_N or on the line width.[17] On the other hand, β-hyperfine coupling constants are known to be highly sensitive to conformational changes.[18] Thus, we chose to focus on the synthesis of β-phosphorylated nitroxides **9** and **10**, which exhibit exo- and intracyclic double bonds (Scheme 1). The EPR features of nitrogen and phosphorus hyperfine coupling constants(a_N and a_P, respectively) were investigated, as well as the kinetics of hydrolysis of **10** into **9** in the presence of various enzymes. The potential of **9** and **10** as polarizing agents was explored through in vitro and in vivo OMRI experiments (Figure 1).

Nitroxide **9** was prepared in eight steps (Scheme 1) starting from the commercially available 2,6-dimethyl-4-hydroxy-hept-1,6-diene **1**. The regioselectivity of the formation of the intracyclic double bond to afford **10**[19] was controlled by using a bulky base, potassium hexamethyldisi-

[*] Prof. G. Audran, L. Bosco, Dr. P. Brémond, Prof. S. R. A. Marque
Aix-Marseille Université, CNRS, ICR, UMR 7273
Case 551, Avenue Escadrille Normandie-Niemen,
13397 Marseille Cedex 20 (France)
E-mail: g.audran@univ-amu.fr
        paul.bremond@univ-amu.fr
        sylvain.marque@univ-amu.fr

Prof. J.-M. Franconi, N. Koonjoo, P. Massot, Dr. P. Mellet,
Dr. E. Parzy, Prof. E. Thiaudière
Centre de Résonance Magnétique des Systèmes Biologiques,
UMR 5536 CNRS, Case 93,
University Bordeaux Segalen
146 rue Leo Saignat, 33076 Bordeaux Cedex (France)
E-mail: jean-michel.franconi@rmsb.u-bordeaux2.fr
        eric.thiaudiere@rmsb.u-bordeaux2.fr

Dr. P. Mellet
INSERM
33076 Bordeaux Cedex (France)
E-mail: philippe.mellet@rmsb.u-bordeaux2.fr
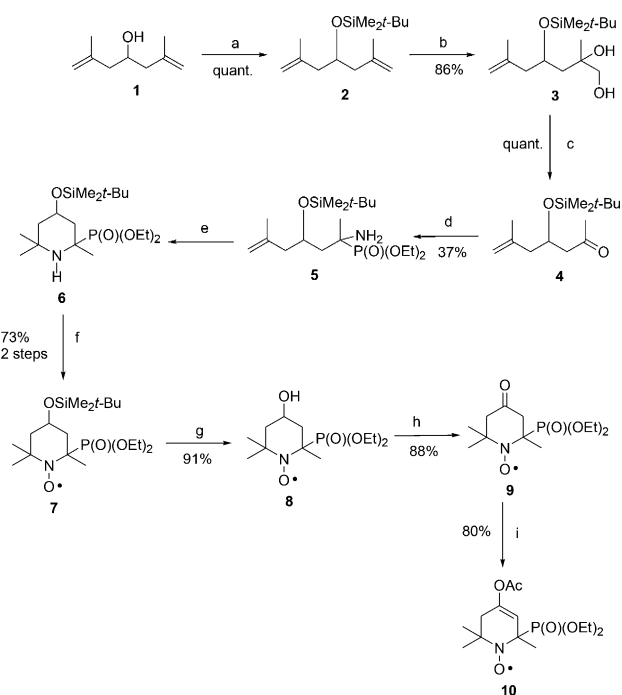
Scheme 1. Preparation of **9** and **10**. a) DMF, imidazole, *tert*-butyldimethylsilyl chloride (TBDMSCl), 5 h, 0 °C; b) (1) OsO$_4$, acetone/water, 15 min, 0 °C; (2) *N*-methylmorpholine-*N*-oxide (NMO), 4 h, 0 °C. c) NaIO$_4$, THF/water (1:3, v/v), 3 h, 0 °C. d) HP(O)(OEt)$_2$, 4Å M.S.. e) (1) Hg(OAc)$_2$, THF/water (1:3, v/v), 30 min, r.t.; (2) NaBH$_4$, NaOH (1 M). f) *meta*-chloroperoxybenzoic acid (*m*CPBA), CH$_2$Cl$_2$, 2 h, 0 °C. g) TBAF, THF, 3 h, 0 °C. h) NMO, TPAP, 4Å M.S., CH$_2$Cl$_2$, 0 °C. i) (1) LiHMDS, THF, 3 h, −80 °C to −45 °C; (2) Ac$_2$O, 2.5 h, −45 °C.
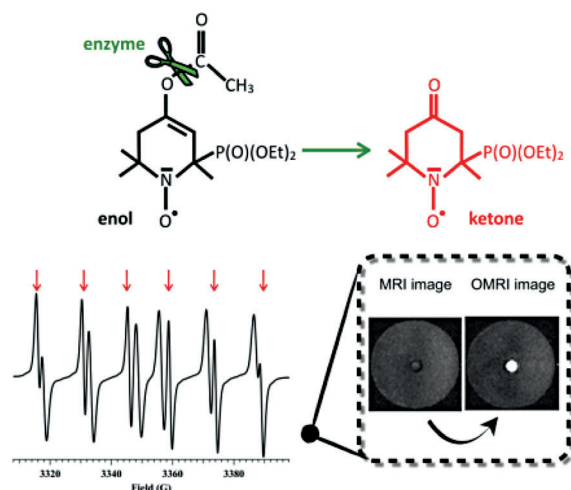

Figure 1. Nitroxides with different EPR signatures to target enzymatic processes with EPR and/or OMRI techniques in vitro and in vivo.

lazane (KHMDS), which reacted with the most acidic protons (see the Supporting Information).

EPR features are reported in Table 1 and Figure 2, and are in very good agreement with previously reported data.[18] Interestingly, nitroxide **10** (intracyclic double bond) exhibits an a_p value 4.4 G smaller than the one of **9** (exocyclic double bond). Moreover, linewidths are narrow enough for OMRI

experiments.[10] Owing to this difference in their a_p values, their spectra are sufficiently resolved to avoid peak overlapping, thus allowing individual quantification of the products in a 1:1 mixture of **9** and **10** (Figure 2).

Table 1: EPR parameters of nitroxides **9** and **10**.

Nitroxides	a_N [G][a]	a_P [G][a]	g[b]	ΔH_{pp} [G][a,c]
9	15.0	43.1	2.0062	1.2
10	15.6	38.7	2.0063	1.8

[a] 1 G = 0.1 mT. [b] Landé's factor. [c] Linewidth peak to peak for the central lines.
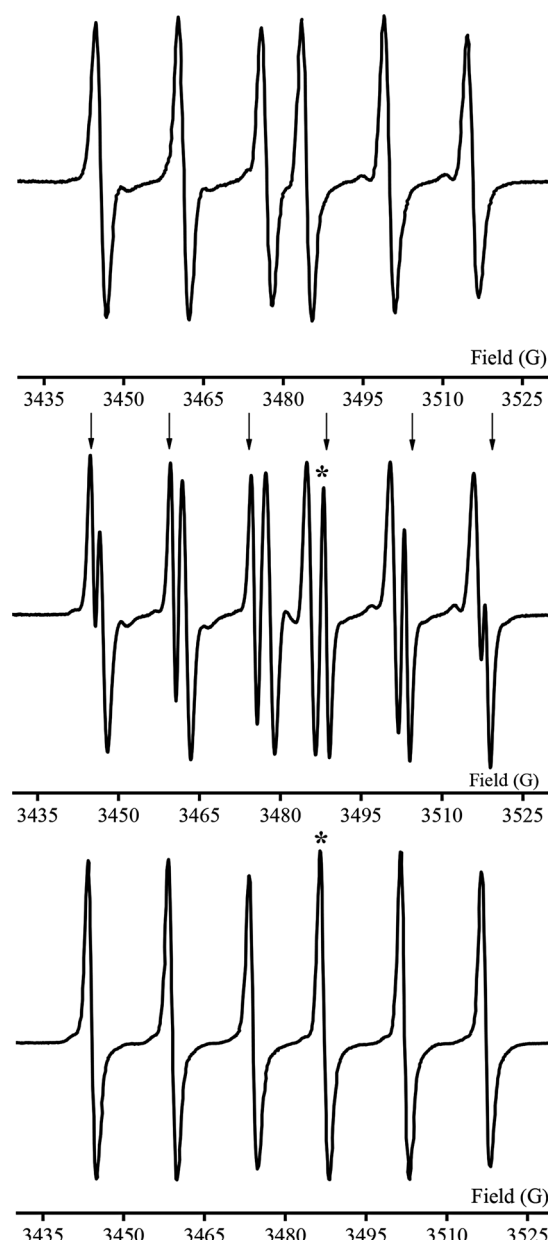

Figure 2. EPR signals of **10** (top) and **9** (bottom) and a 1:1 mixture of **9**/**10** (middle; arrows are for lines of **9**). The starred line in the EPR signal of **9** was used for electronic spin excitation for OMRI.

Enzymatic activity assays were carried out in vitro using the EPR technique to monitor the keto–enol hydrolysis. After an incubation time of 5 h and quantification of the third EPR line for **9**, out of 8 proteases of various specificities and origin, three were able to hydrolyze **10** into **9**, namely, porcine pancreatic elastase (PPE), human neutrophil elastase (HNE) and subtilisin A (Figure 3). Subtilisin A was selected for further experiments because of it displayed the highest activity (95 % hydrolysis in 5 h).
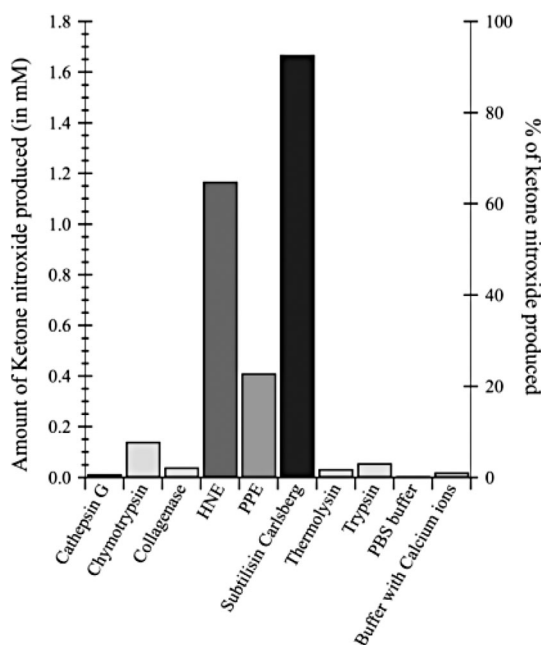

Figure 3. Efficiency of various enzymes as well as of PBS buffer and Ca²⁺ PBS buffer in hydrolysis of 1.8 mM of **10** into **9** for 5 h incubation. *y*-axis in mM (left) and % converted (right).

The kinetics of the consumption of substrate **10** consumption, and the formation of product **9** were monitored to complete hydrolysis (Figre 4). The half-life, $t_{1/2}$ was measured at 74 min with a substrate concentration of 1.1 mM and subtilisin A concentration of 2.8 µM. Given that the Michaelis–Menten condition of $[S] \ll K_M$ was fulfilled at substrate concentrations ranging from 0.3 to 1.1 mM, the catalytic constant, k_{cat}/K_M was 55 M⁻¹ s⁻¹ at 37 °C in saline phosphate buffer pH 7.3. This low value is due to the very partial occupation of the enzyme active site by the small acetyl ligand.[20] The spontaneous hydrolysis rate at 37 °C and pH 7.3 (Figure 4) was not significant during the time of experiment. The rate of increase of **9** in the presence of Eglin C, a natural protease inhibitor from leeches, only showed a slow rate of transformation of **10** into **9** close to the rate of spontaneous hydrolysis, suggesting a complete inhibition of what appears to be a pure enzymatic process.

As already seen above in the EPR spectra, the substrate-to-product conversion revealed a significant coupling shift of about 4 G without line overlapping. This molecular characteristic was then transposed into OMRI applications to monitor enzymatic reactions taking place either in vitro or in vivo. To check whether the non-overlapping condition is valid for
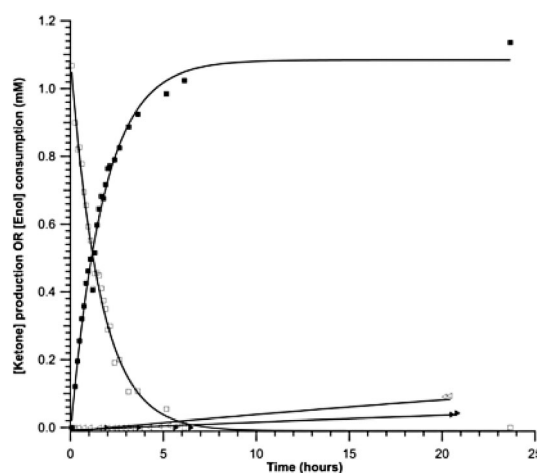

Figure 4. Kinetics for the decay of 1.1 mM of **10** (□) and the generation of **9** (■) in the presence of 2.8 µM of subtilisin A. The generation of **9** in the presence of subtilisin A plus the Eglin C inhibitor (◁), and spontaneous hydrolysis in PBS buffer solution (▶).

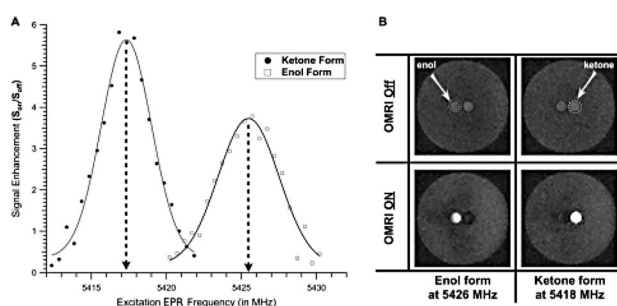*Figure 5.* A) Optimal excitation EPR frequency (in MHz) determination and OMRI signal enhancements for **9** (●) and for **10** (□). B) In vitro spotting of **9** (left inserted tube labeled as enol) and (-)-**10** (right inserted tube labeled as ketone). The first row corresponds to the MRI images without electronic saturation and the second row with electronic saturation.

OMRI, the EPR irradiating frequency was swept for both the substrate and the product. The two spectra are shown in Figure 5 a. 2D images with and without electronic spin saturation were acquired (data not shown) at different equally spaced EPR frequencies ranging from 5412.35 to 5429.85 MHz for **9** and **10** for a proton frequency of 8.24264 MHz. Thus, the maximal signal enhancements were observed at 5417.3 and 5425.3 MHz for **9** and **10**, respectively. As already seen in Table 1, the EPR line width was narrow enough to observe high signal enhancement on the OMRI images and the Δa_P (ca. 8 MHz, Figure 5 a) between the third EPR line of **9** and that of **10** was sufficiently far apart for a selective and distinct electronic EPR saturation for OMRI experiment. In vitro experiments (Figure 5 b) showed that nitroxides **9** and **10** were selectively spotted at 5417.9 MHz and of 5426.2 MHz, respectively. Consequently, OMRI experiments showed that each sample of **9** and **10** was lit up selectively (Figure 5 b). It should be noted that the enhancements observed for **10** were poorer than those for **9**. This result is due to the larger line width of **10** (Table 1).

In vitro OMRI kinetic assays were then carried out to monitor the hydrolysis of (-)-**10** (1.8 mM) in phosphate buffer, pH 7.2 in the presence of subtilisin A (2.8 μM). The rate of production of **9** from (-)-**10** monitored by irradiating the EPR line highlighted in Figure 6 yielded $t_{1/2} = 69$ min. at 37°C, a value fairly close to the one obtained by EPR monitoring. The maximum signal enhancement was found to be 11.3 after 20 h of reaction time. These OMRI data agree with those obtained by EPR.
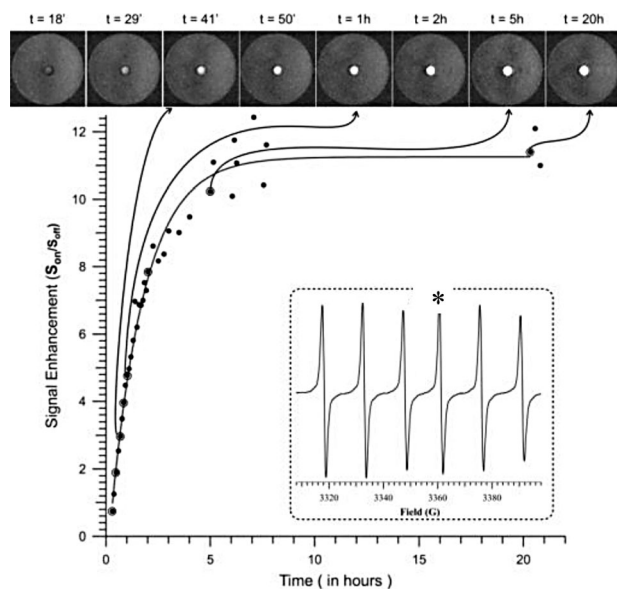

Figure 6. In vitro OMRI monitoring of the hydrolysis of (-)-**10** (1.8 mM) into **9** (bright spot) by subtilisin A (2.8 μM) in phosphate buffer pH 7.2 at 37°C. 2D images were acquired at various time intervals with/without EPR frequency saturation tuned at 5417 MHz. Inset: the starred line in the EPR signal of **9** was used for electronic spin excitation for OMRI.

To definitively highlight the potential of **9** and **10** in probing non-radical enzymatic activity, a mouse was fed with a solution of **10** at 24 mM (see the Supporting Information). Anatomical MRI was first performed and confirmed that the stomach was filled with the nitroxide solution (Figure 7 A). Then, the first 3D OMRI images were acquired with and without electronic EPR saturation of the nitroxides found in the stomach. The saturation frequency was set at 5425.7 MHz and thereby specifically exciting one electronic transition of **10**. A hypersignal with a maximal signal amplification of 5.7 was visible in the stomach, highlighting the presence of the substrate at about 10 min post-gavage (Figure 7 B).

Afterwards, 3D OMRI images were obtained again with and without electronic saturation at the frequency of 5417.5 MHz, corresponding to the equivalent EPR transition line of the product nitroxide **9**. The images revealed that some of the substrate was converted into the ketone product generating a specific high contrast with an 8.5-fold increase at 35 min post-gavage (Figure 7 C). Mouse stomach and intestine pH have been measured at 3 and 5, respectively.[21] The spontaneous hydrolysis of (+)-**10** nitroxide between pH 3 and 7 is not detectable while it is significant at pH of 1 or 9

(Supporting Information, Figure S1). Thus it is the digestive enzymes found in the stomach and/or in the intestine that were able to transform nitroxide **10** into **9**. Clearly, the conformational change from **10** to **9** plays the expected on/off role for selective OMRI experiments affording a powerful tool to investigate in vivo enzymatic processes.

These preliminary results in OMRI show the huge potential of the tautomeric equilibrium between **9** and **10** to investigate non-radical enzymatic processes in vivo using the non-invasive OMRI technique. The primary approach in activity-based molecular imaging has been optical imaging, mainly because of its high sensitivity. MRI is the only one that has high anatomical resolution in 3D, together with no depth limitations and no radiative issues. Furthermore, its poor sensitivity is being handled using the Overhauser effect of **9** and **10** onto the water molecules. In the present study, the signal was enhanced 8.5 times, thus affording a large specific contrast. Here, the in vivo validation was carried out at both substrate and product frequencies using the distinct signatures of each species. Although experiments were performed with only three mice (low statistical reproducibility) and despite that the acetyl nitroxide is a very poor protease substrate compared to usual peptidic substrates, our results confirm unambiguously the feasibility of this approach.

Improvements are still ongoing. Targeting specific disease-related enzymes by grafting enzyme-specific peptides on **10** is expected to enhance k_{cat}/K_M by several orders of magnitude, thus providing both sensitivity and protease specificity.[22]

Proteases are tightly regulated biomolecules involved in many physiological events, and deregulations in their activities are correlated to various diseases, such as cancer with overwhelming matrix metalloproteinase (MMP) activity, pancreatitis with premature in situ pancreatic protease activation, cystic fibrosis, or chronic obstructive pulmonary disease (COPD) with overwhelming concentration of neutrophil proteases, and multiple sclerosis and rheumatoid arthritis with deleterious MMP activity. The specific nitroxides and imaging technique described here would certainly help for better understanding the function of those overexpressed proteases and their sustaining activities in vivo through monitoring and disease localization. Eventually, drug design against those proteases could also be tested accordingly.

Consequently, there is a need to develop such an application for humans. At 0.2 T Tesla, the 5.5 GHz waves corresponding to the resonance frequency of the electron is suitable for small animals but not for humans because of the poor penetration into tissues. However, it is possible at very low field. For instance, at earth field the electron resonance frequency is about 60 MHz, a usual frequency in clinical MRI. For connection to the anatomical images, two possibilities arise: a field cycling apparatus[23] or more sensitive detectors.[24] As a consequence much higher Overhauser enhancements are predicted[25] and hence a much lower detection limit of the nitroxides.

These nitroxides are also suitable for a broad range of enzymes as the ester moiety can be designed for a particular enzyme, such as by using specific peptides, sugars, or lipids.
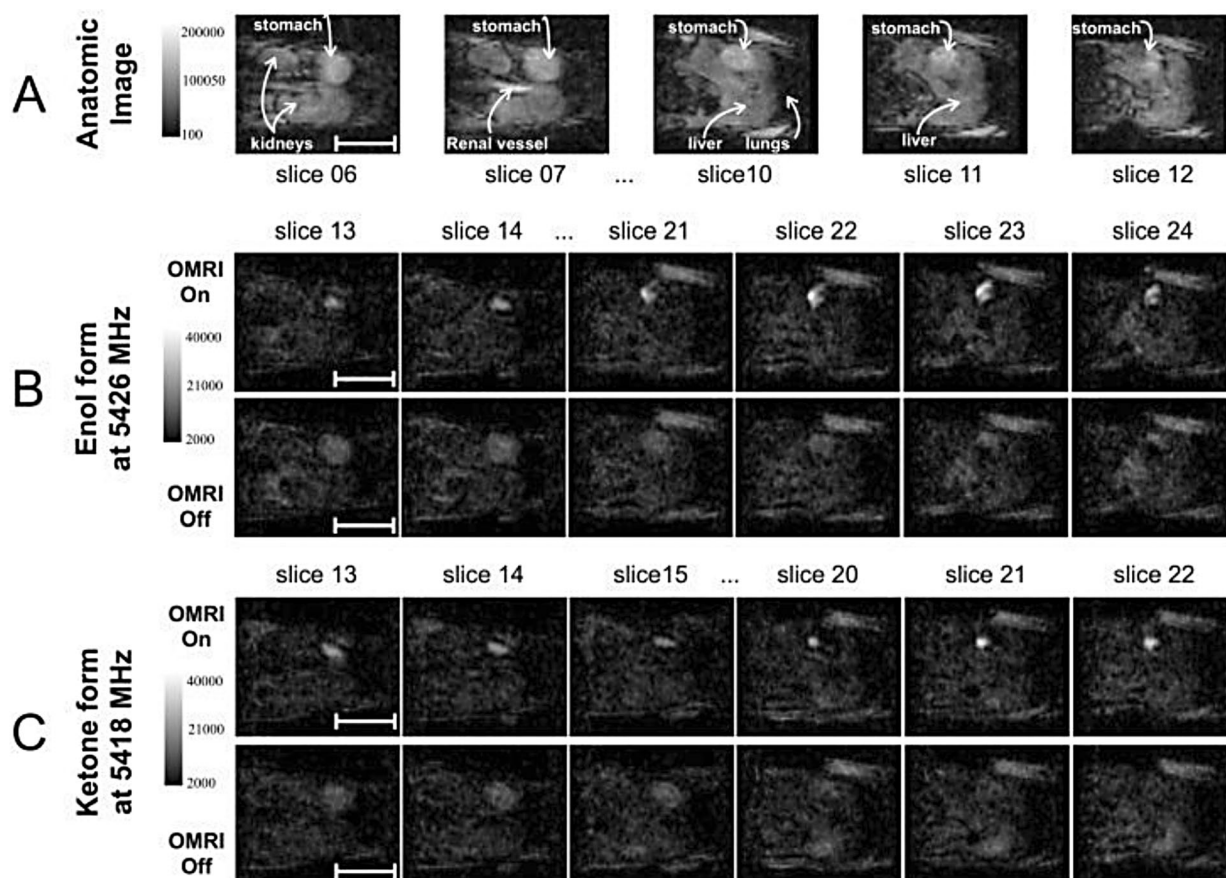
Figure 7. A) 3D anatomical MRI image of the stomach. B) The first row corresponds to the image with electronic saturation at 5425.7 MHz and the slices in the second row are the corresponding non-saturated electronic spins. C) The first row corresponds to the image with an electronic saturation of 5417.5 MHz (first row) and without (second row). All OMRI images were acquired in 18 seconds and then reconstructed into an isotropic spatial resolution of 0.5 mm in all three directions. The anatomical image has a spatial resolution of $0.5 \times 0.54 \times 1$ mm^3 and a temporal resolution of about 3.5 min.

These non-exhaustive biomolecules, once grafted onto the nitroxide moiety, can be applied to several enzyme-specific studies including quantification, kinetic constant determination, and drug inhibition tests.[22]

[1] A. Zagdoun, G. Casano, O. Ouari, M. Schwarzwalder, A. J. Rossini, F. Aussenac, M. Yulikov, G. Jeschke, Ch. Copéret, A. Lesage, P. Tordo, L. Emsley, *J. Am. Chem. Soc.* **2013**, *135*, 12790–12797.

[2] L. Zhu, J. Xie, M. Swierczewska, F. Zhang, Q. Quan, Y. Ma, X. Fang, K. Kim, S. Lee, X. Chen, *Theranostics* **2011**, *1*, 18–27.

[3] P. Habibollahi, J. L. Figueiredo, P. Heidari, A. M. Dulak, Y. Imamura, A. J. Bass, S. Ogino, A. T. Chan, U. Mahmood, *Theranostics* **2012**, *2*, 227–234.

[4] V. Catanzaro, C. V. Gringeri, V. Menchise, S. Padovan, C. Boffa, W. Dastrù, L. Chaabane, G. Digilio, S. Aime, *Angew. Chem. Int. Ed.* **2013**, *52*, 3926–3930; *Angew. Chem.* **2013**, *125*, 4018–4022.

[5] N. Guyot, J. Wartelle, L. Malleret, A. A. Todorov, G. Devouassoux, Y. Pacheco, D. E. Jenne, A. Belaaouaj, *Am. J. Pathol.* **2014**, *184*, 2197–2210.

[6] D. Grucker, *Magn. Reson. Med.* **1990**, *14*, 140–147.

[7] K. Golman, J. S. Petersson, J. H. Ardenkjaer-Larsen, I. Leunbach, L. G. Wistrand, K. Ehnholm, K. Liu, *J. Magn. Reson. Imaging* **2000**, *12*, 929–938.

[8] E. Parzy, V. Bouchaud, P. Massot, P. Voisin, N. Koonjoo, D. Moncelet, J.-M. Franconi, E. Thiaudière, P. Mellet, *PLoS One* **2013**, *8*, 2.

[9] N. Koonjoo, E. Parzy, P. Massot, M. Lepetit-Coiffé, S. R. A. Marque, J.-M. Franconi, E. Thiaudière, P. Mellet, *Contrast Media Mol. Imaging* **2014**, *9*, 363–371.

[10] P. Mellet, P. Massot, G. Madelin, S. R. A. Marque, E. Harte, J.-M. Franconi, E. Thiaudière, *PLoS One* **2009**, *4*, e5244.

[11] A. R. Forrester, F. A. Neugebauer, *Organic N-Centered Radicals and Nitroxide Radicals*, Landolt-Börnstein: *Molecules and Radicals*, *Vol. 9*, *Part c1* (Ed.: H. Fischer), Springer, Heidelberg, **1979**.

[12] A. R. Forrester, *Nitroxide Radicals*, Landolt-Börnstein: *Molecules and Radicals*, *Vol. 17*, *Part d1,d2* (Ed.: H. Fischer), Springer, Heidelberg, **1989**.

[13] O. V. Efimova, Z. Sun, S. Petryakov, E. Kesselring, G. L. Caia, D. Johnson, J. L. Zweier, V. V. Khramtsov, A. Samouilov, *J. Magn. Reson.* **2011**, *209*, 227–232.

[14] A. Samouilov, O. V. Efimova, A. A. Bobko, Z. Sun, S. Petryakov, T. D. Eubank, D. G. Trofimov, I. A. Kirilyuk, I. A. Grigor′ev, W. Takahashi, J. L. Zweier, V. V. Khramtsov, *Anal. Chem.* **2014**, *86*, 1045–1052.

[15] A. Alberti in *Nitroxide Radicals and Nitroxide Based High-Spin Systems*, Landolt-Börnstein: *Molecules and Radicals*, *Vol. 26*, *Part D* (Ed.: H. Fischer), Springer, Heidelberg, **2005**.

[16] W. Takahashi, A. A. Bobko, I. Dhimitruka, H. Hirata, J. L. Zweier, A. Samouilov, V. V. Khramtsov, *Appl. Magn. Reson.* **2014**, *45*, 817–826.

[17] V. V. Khramtsov, J. L. Zweier, *Functional in vivo EPR Spectroscopy and Imaging Using Nitroxide and Trityl Radicals*, Stable Radicals: *Fundamentals and Applied Aspects of Odd-Electron Compounds* (Ed.: R. G. Hicks), Wiley, Chichester, **2010**, pp. 537–566.

[18] G. Audran, L. Bosco, P. Brémond, T. Butscher, S. R. A. Marque, *Appl. Magnet. Reson.* **2015**, DOI: 10.1007/s00723-015-0649-4.

[19] Some amounts of **10** were separated on chiral HPLC to yield (+)-**10** and (-)-**10**.

[20] However, using enol esters of protease-specific peptides as substrate should easily enhance this catalytic constant k_{cat}/K_M 10^3 to 10^4 times. Work in progress.

[21] E. L. McConnell, A. W. Basit, S. Murdan, *J. Pharm. Pharmacol.* **2008**, *60*, 63–70.

[22] G. Audran, L. Bosco, P. Brémond, J.-M. Franconi, S. R. A. Marque, P. Massot, P. Mellet, E. Parzy, E. Thiaudière, E.U. EP15306115.5.

[23] P. J. Ross, L. M. Broche, D. J. Lurie, *Magn. Reson. Med.* **2015**, *73*, 1120–1124.

[24] V. S. Zotev, T. Owens, A. N. Matlashov, I. M. Savukov, J. J. Gomez, M. A. Espy, *J. Magn. Reson.* **2010**, *207*, 78–88.

[25] T. Guiberteau, D. Grucker, *J. Magn. Reson. Ser. B* **1996**, *110*, 47–54.

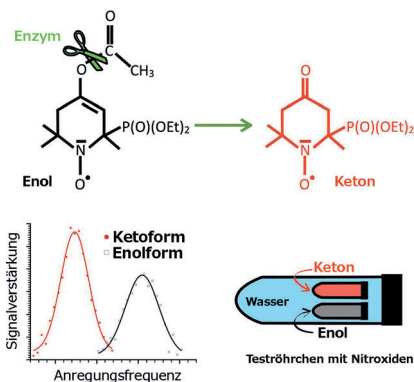## Zuschriften

G. Audran,* L. Bosco, P. Brémond,*
J.-M. Franconi, N. Koonjoo,
S. R. A. Marque,* P. Massot, P. Mellet,*
E. Parzy, E. Thiaudière* —— ▮▮▮▮–▮▮▮▮

Enzymatically Shifting Nitroxides for EPR
spectroscopy and Overhauser-Enhanced
Magnetic Resonance Imaging

In-vivo-Bildgebung von Protease: Enzymatisch aktivierte Nitroxide können durch EPR-Spektroskopie und eine Overhauser-verstärkte MRI-Technik aufgezeichet und nachverfolgt werden. Die Methodenkombination ermöglicht die Visualisierung der Proteaseaktivität in vivo im Verdauungstrakt von Mäusen.